PHYSICAL REVIEW C VOLUME 25, NUMBER 2 FEBRUARY 1982

Proton-induced muon production from nuclei

D. L. Weiss*
Physics Department, Indiana University, Bloomington, Indiana 47401
and Group T-5, Los Alamos Scientific Laboratory, Los Alamos, New Mexico 87544

G. E. Walker†
Institute for Nuclear Theory and Physics Department, FM-15,
University of Washington, Seattle, Washington 98195
and Physics Department, Indiana University, Bloomington, Indiana 47401
(Received 24 August 1981)

We study the weak proton-induced muon production reaction using the impulse approximation. The process is studied below threshold for real pion production assuming a ^{12}C target. The theoretical predictions for muon angular distributions are given for the ground state, low-lying excited states, and the energetically available nuclear continuum. The process is a very rare event using presently available beam intensities. We argue that corrections to the impulse approximation are expected to be important and indicate how to use partial conservation of axial vector current and experimental (p,π) results to obtain more reliable estimates. The reaction can be a rich additional source of information regarding the relationship between the many-body pion source current and the space and time components of the nuclear axial current. Even with the conjectured substantial increase over the impulse approximation, the subthreshold counting rate seems too low for detailed experimental investigation at this time. A simple exploratory experiment starting above pion threshold and working downward in energy is suggested.

[NUCLEAR REACTIONS $^{12}C(p,\mu^+\nu)^{13}C$, $E_p \simeq 148$ MeV, calculated $\sigma(\theta)$ and σ_T impulse approximation, PCAC extensions.]

I. INTRODUCTION

In the past few years there has been increasing interest in the connection between the nuclear many-body axial-vector current, isobar and pionic degrees of freedom, and rescattering in the nucleus.[1] The purpose of the present paper is to illustrate how proton-induced muon production could contribute to the general study of the many-body hadronic weak currents, and to estimate the cross section of this relatively rare event in the impulse approximation. We also discuss how to go beyond the impulse approximation, making the connection between nuclear pion production (p,π) processes to obtain the hadronic weak axial vector current required in muon production. Since medium energy large momentum transfer pion and photoproduction processes are only partially understood, one could also argue that eventually muon production could contribute to the better understanding of these processes. Given the present seeming complexity of the situation regarding the role of pionic and isobar degrees of freedom in various processes, additional sources of information (to be sure possessing their own intrinsic uncertainties) should be useful to explore.

The basic weak process we consider is

$$p + {}_ZA^N \rightarrow {}_ZA^{N+1} + \mu^+ + \nu \,. \tag{1}$$

This process might be studied, initially, below threshold for real pion production so that decay muons from this strong interaction do not swamp the observed counts. Thus, to study muon production experimentally requires an *intense* beam of $\sim 100-140$ MeV protons (after consideration of center-of-mass and binding effects) as are becoming available at intermediate energy facilities such as the Indiana University Cyclotron Facility (IUCF). The basic production reaction is a weak interaction (inverse muon capture), thus considerations involving the weak vector and axial vector

currents in the nucleus are relevant. Moreover, since the process delivers high momentum transfer $\gtrsim 400$ MeV/c to the nucleus (while requiring information regarding the weak hadronic current at low momentum transfer $\vec{q} \lesssim 100$ MeV/c and $q_0 \approx m_\mu$), two nucleon mechanisms (TNM) such as virtual intermediate isobars as in pion production and high q photoabsorption must eventually be considered.[2] To a large extent the same diagrams included for the renormalization of g_A and discussing exchange currents in electromagnetic processes are also relevant for the discussion of TNM for threshold pion production and muon production. In this introductory study we concentrate on the impulse terms and use experimental data on (p,π) to estimate the order of magnitude of multinucleon processes.

In the next section we present the basic formulas needed to calculate muon production using the impulse approximation and a limiting "model" application of partial conservation of the axial vector current of (PCAC). The actual calculations are for muon production on ^{12}C leading to bound states of ^{13}C and low lying single neutron states in the continuum. For actual experiments, nuclei in the Fe, Ni region are preferred to avoid contamination due to pions produced and decaying into muons from materials in the beam line, etc., with lower threshold than ^{12}C.

In Sec. III the results of the calculations in carbon are given and discussed. The importance of using realistic single particle orbitals for calculating high momentum transfer processes is emphasized. We note the sensitivity of the results to such uncertainties is significantly diminished in pion production when a two nucleon mechanism is adopted.[2] Adopting a carbon target thickness of 150 mg/cm^2 and a 148 MeV, 10 μA proton beam results in a relatively rare total muon production counting rate of ~ 1 count/decade. However, an estimate based on a simple application of PCAC and use of pion production data suggests that the actual counting rate could be more than an order of magnitude larger.

Finally, in Sec. IV we summarize and discuss our impulse approximation results. A more involved calculation, including the TNM is motivated. Such estimates should follow a quantitatively successful calculation of (p,π). The study of (p,μ^-) which is forbidden in the impulse approximation, analogous to (p,π^-) in pion production, would play an important role in establishing the importance of a two nucleon mechanism.

II. MUON PRODUCTION FORMULAS

In the impulse approximation the muon production reaction, Eq. (1), can be calculated using the usual current-current interaction for weak processes. The cross section, for an unpolarized incident proton leading to a particular final state, is given by

$$d\sigma = \tfrac{1}{2} \sum_{\text{spins}} \int d^3K_f \frac{d^3k_\nu}{(2\pi)^9} d^3k_\mu \, |\langle f|S|i\rangle|^2 \frac{E_p}{k_p} , \tag{2}$$

where K_f, k_ν, and k_μ denote the final nuclear target, neutrino, and muon momenta, respectively, in the laboratory. The S matrix operator is obtained from the weak Hamiltonian density via

$$S = -i \int d^4x \, H_w(x) , \tag{3}$$

where

$$H_w(x) = -\frac{G}{\sqrt{2}} \mathcal{J}_\lambda^{(+)} \mathcal{J}^{(-)\lambda} \tag{4}$$

and

$$\mathcal{J}_\lambda = J_\lambda(\text{hadronic}) + j_\lambda(\text{leptonic}) . \tag{5}$$

The leptonic current is related to the leptonic field operators in the usual V-A theory

$$j_\lambda^{(-)}(x) = \bar{\psi}_\mu(x)[\gamma_\lambda(1-\gamma_5)]\psi_\nu(x) , \tag{6}$$

where the field operators are defined in Ref. 3. The hadronic weak current is complicated by the strong interaction and is given, in general, by

$$J_\lambda^{(-)}(x) = \bar{\psi}_n(x)[F_1\gamma_\lambda + F_2\sigma_{\lambda\nu}q^\nu + F_S q_\lambda + F_A\gamma_5\gamma_\lambda + F_p\gamma_5 q_\lambda + F_T\gamma_5\sigma_{\lambda\nu}q^\nu]\psi_p(x)$$

($q \equiv$ four momentum transfer) . (7)

The weak hadronic current is evaluated at *low* momentum transfer in sub-pion-threshold muon production, and so for this initial estimate we retain the dominant vector (F_1) and axial vector (F_A) terms. In the impulse approximation the values of F_1 and F_A are taken as the free nucleon values. Because nonrelativistic final neutron wave functions will be used, it is necessary to make a nonrelativistic reduction of the weak hadronic current. The results for the vector current are

$$\lambda = 0 \; J_{V0}^{(-)} = F_1 \delta_{S_N S_p} , \tag{8a}$$

$$\lambda \neq 0 \; J_{V\lambda}^{(-)} = -\frac{F_1}{2M}(\vec{k}_p + \vec{k}_n)_\lambda \delta_{S_N S_p} + \frac{iF_1}{2M} \chi_{S_N}^{+}(\vec{\sigma}\times\vec{q})_\lambda \chi_{S_p} , \tag{8b}$$

while for the axial vector current

$$\lambda=0\ J_{A0}^{(-)}=-\frac{F_A}{2M}\chi_{S_N}^{+}[\vec{\sigma}\cdot(\vec{k}_p+\vec{k}_n)]\chi_{S_p}\ , \tag{9a}$$

$$\lambda\neq 0\ J_{A\lambda}^{(-)}=F_A\chi_{S_N}^{+}(\sigma_\lambda)\chi_{S_p}\ , \tag{9b}$$

where the χ are the hadronic spin functions and the $k_{n,p}$ denote the single nucleon momentum. Note since the (impulse) axial vector current time component contains a $\vec{k}/M$ reduction it is quite small for events involving initial and final bound nucleons. We shall see later that as one goes away from the impulse approximation, the time component becomes relatively much more important. Of course even in the impulse approximation velocity terms can be important for ~ 150 MeV incident nucleons.

We assume an initial nonrelativistic hadronic state

$$|k_i\rangle=\sqrt{\xi}e^{i\vec{k}'_p\cdot\vec{r}'}\chi_{S_p}\phi_T e^{i\vec{K}_i\cdot\vec{R}_{\text{c.m.}}}e^{-iE_i t}\ ,$$

$$(r'\equiv r_{\text{lab}}-R_{\text{c.m.}})\ , \tag{10}$$

where $\sqrt{\xi}e^{i\vec{k}'_p\cdot\vec{r}'}$ is the incident medium energy proton relative coordinate wave function with absorption reduction factor $\sqrt{\xi}$. It has been observed that in the energy region 130–200 MeV the main effect of the proton optical potential is to cause a *slight* decrease in the available flux with only small momentum dispersion effects. For our actual numerical calculations for a 148 MeV proton on ^{12}C we use $\xi=0.55$.[4] (See later discussion.) In Eq. (10), ϕ_T denotes the original A particle intrinsic ground state wave function, while $e^{i\vec{K}_i\cdot\vec{R}_{\text{c.m.}}}$ is the initial $A+1$ center-of-mass wave function with K_i measured in the laboratory system. The final nonrelativistic hadronic state, assuming a single lsj coupled neutron bound outside a closed shell target, is given by

$$|k_f\rangle=\int\frac{d^3K}{(2\pi)^{3/2}}e^{i\vec{K}\cdot\vec{r}'}\phi_{Nlj_z}(\vec{K})$$

$$\times\phi_T e^{i\cdot\vec{K}_f\cdot\vec{R}_{\text{c.m.}}}e^{-iE_f t}\ , \tag{11a}$$

where

$$\phi_{Nlj_z}(r')=\int d^3K\,e^{i\vec{K}\cdot\vec{r}'}(2\pi)^{3/2}\phi_{Nlj_z}^{(\vec{K})}\ , \tag{11b}$$

$$\phi_{Nlj_z}(r')=\sum_{s_{zn}l_{zn}}(l_n l_{zn}\tfrac{1}{2}s_{zn}\,|\,j_n j_{zn})$$

$$\times\chi_{s_{zn}}\phi_{Nl_n l_{zn}}^{(r')}\ . \tag{11c}$$

Now we combine the expressions above to obtain the expression for the cross section. Note we detect only the final muon, thus we wish $d^2\sigma/d\Omega_\mu dE_\mu$. Using

$$d^3k_\mu=k_\mu{}^2dk_\mu d\Omega_\mu,\quad dk_\mu=\frac{E_\mu}{k_\mu}dE_\mu \tag{12}$$

one obtains from Eq. (2), carrying out integrations over $R_{\text{c.m.}}$ and t

$$\frac{d^2\sigma}{d\Omega_\mu dE_\mu}=\tfrac{1}{2}\sum_{\substack{s_p,j_{zn}\\ s_\nu,s_\mu}}\int d^3k_\nu\frac{d^3k_F}{(2\pi)^9}\frac{E_p}{|k_p|}E_\mu k_\mu w_{fi}\ , \tag{13}$$

where

$$w_{fi}\equiv\frac{|S|^2}{\text{vol time}}$$

$$=\frac{G^2}{2}\frac{m_\mu}{E_\mu 2\omega_\nu}(2\pi)^3(2\pi)^4\delta(E_f-E_i)$$

$$\times\delta(\vec{P}_f-\vec{P}_i)\tilde{l}^\lambda\tilde{l}^{\sigma *}J_\lambda J_\sigma^*\ . \tag{14}$$

The $\tilde{l}$ operators contain the traces over the lepton operators. The J's contain the hadronic operators and are defined below. We rewrite Eq. (14) in the form

$$\frac{d^2\sigma}{d\Omega_\mu dE_\mu}=\frac{1}{8}\frac{E_p}{|k_p|}\frac{k_\mu m_\mu}{(2\pi)^2}G^2$$

$$\times\sum_{s_p j_{zn}}\int d^3k_\nu\frac{d^3k_F}{\omega_\nu}\delta(E_f-E_i)$$

$$\times\delta(\vec{P}_f-\vec{P}_i)\eta^{\lambda\sigma}J_\lambda J_\sigma^*\ , \tag{15}$$

where

$$\eta^{\lambda\sigma}=\text{tr}\left[\gamma^\lambda(1-\gamma_5)\frac{(\not{k}_\mu-m_\mu)}{2m_\mu}\gamma^\sigma(1-\gamma_\sigma)\not{k}_\nu\right]\ , \tag{16}$$

where $\not{k}\equiv\gamma_\alpha k^\alpha$. We have used a computer program CNETA to evaluate the lepton traces and have checked the results by hand. The hadron contributions $J_\lambda J_\sigma^*$ are more tedious to compute but can be obtained from $J^{V,A}$. For vector

$$J^{v}_{\lambda}=F_1\sum_{1_{2n}}\phi^{*}_{Nll_{zn}}(\vec{K}_F-\vec{k}_p/(A+1))(1_n 1_{zn}\tfrac{1}{2}s_p\,|\,jj_{zn}),\ (\lambda=0)\text{ ,time ,} \tag{17a}$$

$$=-\frac{F_1}{2m}Q\lambda\sum_{l_{zn}}\phi^{*}_{nll_{zn}}(\vec{K}_F-\vec{k}_p/(A+1))(l_n l_{zn}\tfrac{1}{2}s_p\,|\,jj_{zn})\text{ ,}$$

$$+\sqrt{12}\frac{F_1}{2m}\sum_{\substack{l_{zn}\\ s_z}}\sum_{\alpha_1\alpha_2}\phi^{*}_{Nll_{zn}}(\vec{K}_F-\vec{k}_p/(A+1))(-1)^{1/2-s_z}(l_n l_{zn}\tfrac{1}{2}s_z\,|\,jj_{zn})$$

$$\times(1\alpha_1 1\alpha_2\,|\,1\lambda)\begin{pmatrix}\frac{1}{2} & 1 & \frac{1}{2}\\ -s_z & \alpha_1 & s_p\end{pmatrix}q_{\alpha_2},\ (\lambda=1,2,3,),\text{ space .} \tag{17b}$$

For axial vector,

$$J^{A}_{\lambda}=\frac{\sqrt{18}}{2m}F_A\sum_{l_{zn}s_z}\sum_{\alpha_1\alpha_2}\phi^{*}_{Nll_{zn}}(\vec{K}_F-\vec{k}_p/(A+1))$$

$$\times(l_n l_{zn}\tfrac{1}{2}s_z\,|\,jj_{zn})(-1)^{1/2-s_z}(1\alpha_1 1\alpha_2\,|\,00)\begin{pmatrix}\frac{1}{2} & 1 & \frac{1}{2}\\ -s_z & \alpha_1 & s_p\end{pmatrix}Q_{\alpha_2},\ (\lambda=0),\text{ time ,} \tag{17c}$$

$$=\sqrt{6}F_A\sum_{l_{zn}s_z}\phi^{*}_{Nll_{zn}}(\vec{K}_F-\vec{k}_p/(A+1))(-1)^{1/2-s_z}(l_n l_{zn}\tfrac{1}{2}s_z\,|\,jj_z)$$

$$\times\begin{pmatrix}\frac{1}{2} & 1 & \frac{1}{2}\\ -s_z & \lambda & s_p\end{pmatrix},\ (\lambda=1,2,3),\text{ space ,} \tag{17d}$$

Here $\vec{q}\equiv\vec{k}_p-\vec{K}_F$ and $\vec{Q}\equiv\vec{K}_F+(A-1/A+1)\vec{k}_p$ with $\vec{k}_p(\vec{K}_F)$ the initial (final) proton ($A+1$ target) laboratory momentum. We note that momentum conservation requires $\vec{k}_\mu+\vec{k}_\nu+\vec{K}_F=\vec{k}_p$ and k_μ and k_ν are relatively small (see next section), thus $|\vec{q}|\lesssim 100$ MeV/c, while $|\vec{Q}|\gtrsim 400$ MeV/c. Therefore we are using the weak hadronic form factors F_1 and F_A, etc., at low momentum transfer where, in the free case, they are relatively well known. On the other hand the nuclear wave function $\phi(K)$ is being evaluated at momentum transfers significantly above the Fermi momentum which means that uncertainties in the single particle orbitals and the possibility of two step processes are factors.

The delta functions which determine energy and momentum conservation are given by

$$\delta(E_f+\omega_\nu+E_\mu-E_i)\delta^3(\vec{K}_F+\vec{k}_\nu+\vec{k}_\mu-\vec{k}_p)\ . \tag{18}$$

All of the quantities appearing in Eq. (18) are defined in the laboratory system. We use nonrelativistic kinematics for the energy-momentum relationship of the final nuclear target, all other particles are treated relativistically. More specifically

$$\begin{aligned}E_F&=M^{\text{g.s.}}_{A+1}+E_{\text{ex}}+\frac{K_F{}^2}{2M_{A+1}}\ ,\\ E_i&=M_A+E_{\text{proton}}\ ,\\ \omega_\nu&=|\vec{k}_\nu|\ ,\\ E_\mu&=\sqrt{m_\mu{}^2+k_\mu{}^2}\ .\end{aligned} \tag{19}$$

As a result of the initial conditions and because of the detection of the final muon with assumption of a definite given final state of the nucleus, the unknowns are $\vec{k}_\nu$, ω_ν, $\vec{K}_F$, and $\vec{K}_F{}^2/2M_{A+1}$. The energy conservation delta function is used to eliminate ω_ν

$$\omega_\nu=A-\frac{K_F{}^2}{2M_{A+1}},\quad A=M_A+E_p-E_\mu-M^{\text{g.s.}}_{A+1}-E_{\text{ex}}\ . \tag{20}$$

The three dimensional momentum delta function is used to eliminate K_F in terms of k_p, k_μ, and k_ν. Squaring yields

$$K_F^2 = K_F^2(k_p, k_\mu, k_\nu) = B^2 - 2\left[A - \frac{K_F^2}{2M_{A+1}}\right]\left[\frac{\vec{k}_\nu}{\omega_\nu}\cdot\vec{B}\right] + \left[A - \frac{K_F^2}{2M_{A+1}}\right]^2 , \quad (21)$$

where $B \equiv (\vec{k}_p - \vec{k}_\mu)$. From Eqs. (18) and (21) it can be seen that both E_F and $\vec{K}_F$ are functions of the direction of the neutrino momentum direction. In the actual calculations we numerically carry out the integration over the neutrino direction and use the appropriate $\vec{K}_F$ and K_F^2 for the given neutrino direction grid point. The parameters adopted for the ^{12}C muon production calculation include $m = 938.2796$ MeV, $m_\mu = 105.659$ MeV, $G = (1.023/m^2) \times 10^{-5}$ $F_A = 1.21$. For the generation of the final bound state neutron wave function a Saxon-Woods single particle potential was adopted. Assuming a central potential of the form

$$V = \frac{V_0}{1 + e^{-(r-R)/a}} , \quad (22)$$

the parameters $R = 1.31\, A^{1/3} F$ and $a = 0.5\, F$ have been utilized.[5] The well depth V_0 is determined by fixing the binding energy of the orbital under consideration by using experimental energy levels. The spin-orbit potential is chosen to give a $1p_{1/2}$-$1p_{3/2}$ splitting of 6 MeV.

For positive energy single neutron orbitals a Saxon-Woods single particle potential with the same parameters given above was utilized. In this case, the well depth is chosen as 55 MeV and the positive energy eigenvalue is determined by numerically solving the Schrödinger equation. We have ensured that low energy resonant l values included as bound state wave functions have not been included in the continuum contribution. For the continuum calculation an extra $\int dk_n/(2\pi)^3$ factor should be included in Eq. (13). The continuum low energy neutron is treated nonrelativistically. The procedure for normalizing the continuum functions and carrying out the resulting numerical calculations is given in Ref. 6.

In obtaining the formulas for muon production contained in this section we have assumed plane waves for the initial proton and final muon wave functions. Fortunately, in the energy region of interest the main effects of distortion can be easily included. In the case of the $T_p^{\text{lab}} \simeq 150$ MeV proton, the most important effect is a general reduction of the cross section due to absorption (the real part of the optical potential is near zero in this region). In their studies of (γ,p) reactions, Londergan and Nixon[4] have assumed modified plane waves of the form $\sqrt{\xi}e^{ip'r}$, where

$$p' = \sqrt{p^2 + 2\mu(\bar{V} + i\bar{W})} . \quad (23)$$

By comparing the distorted waves generated from phenomenological optical potentials to those obtained via the modified plane waves they have obtained, near 150 MeV $\xi = 0.55$ with only very minor modifications in the phase $k \to p'$, since the main effects of absorption are already contained in ξ. Thus, in the following, we adopt the overall renormalization factor 0.55 due to incident proton absorption. The extra complexity of more realistic proton distorted waves is expected to have a minor effect on total muon production rates [as in the case of large momentum transfer, medium energy (γ,p) processes].

The main effect in muon wave function distortion arises from the Coulomb potential felt by the muon. For positively (negatively) changed muons, this results in a reduction (enhancement) in the muon wave function in the region of the nucleus. An accurate quantitative estimate of this effect can be obtained by studying the general solution for the muon wave function, given by[7]

$$u_c = \Gamma(1+in)e^{-(n\pi)/2}e^{i\vec{k}\cdot\vec{r}} \times F(-in, 1, 2ik_\mu r \sin^2\theta/2) , \quad (24)$$

where

$$F(a,b,X) = 1 + \frac{aX}{b\,1!} + \frac{a(a+1)X^2}{b(b+1)2!} + \cdots \quad (25a)$$

and

$$n = \frac{ZZ'}{137}\frac{c}{v} . \quad (25b)$$

In the region where the production rate is non-negligible, the muon momentum, k_μ, varies from 30 to 90 MeV/c. For ^{12}C, $Z = 6$ and the radius of the nuclear matter distribution has $r_{\max} \sim 3$ fm. Thus we obtain $F \sim 1$ in the region of interest. (Note

$$nk_\mu r \lesssim 6/137 r_{\max} \frac{[(106)^2 + \hbar^2 k_\mu^2 c^2]^{1/2}}{\hbar c} \lesssim 0.1 .$$

and, in the next section, we find the production

cross section is forward peaked.) The appropriate renormalization factor, for the approximation adopted here, i.e., $F=1$ is obtained from

$$\beta_{k_\mu}=\left|\frac{u_c}{e^{i\vec{k}_\mu\cdot\vec{r}}}\right|^2=\frac{2n\pi}{e^{2n\pi}-1}\ , \tag{26}$$

where, as examples, $\beta=(0.437, 0.713, 0.790)$ for $k_\mu=(20, 50, 80\ \mathrm{MeV}/c)$, respectively. The theoretical cross sections reported in Sec. III have been obtained including the renormalization factor $\xi\beta_{k_\mu}$ in the calculations.

There has been considerable discussion[1] regarding the connection between the nuclear axial current and the many body system pionic properties. By using the PCAC relation between the nuclear axial current and the nuclear pion field operator, i.e.,

$$\partial^\mu A_\mu(x)=f_\pi m_\pi{}^2\phi(x)\ , \tag{27}$$

(f_π is the charged pion decay constant $f_\pi=0.94\ m_\pi$), one can, depending on the four momentum transfer region where A_μ is required and a model for the nuclear pion field, go considerably beyond the impulse approximation for A_μ. For example, in the region $q_0\simeq 0$, such as in nuclear β decay, for infinite nuclear matter[8]

$$\vec{A}(\vec{q})=\sum_i\left[-F_A\eta\vec{\sigma}_i+f_\pi\frac{g_r}{2m_{\mathrm{nuc}}}\times\frac{(1+\alpha)\vec{q}(\vec{\sigma}_i\cdot\vec{q})}{(1+\alpha)\vec{q}^2+m_\pi{}^2}\right] \tag{28}$$

allowing one to define effective axial vector, $(F_A)_{\mathrm{eff}}$, and induced pseudoscalar coupling constants, $(F_p)_{\mathrm{eff}}$, where

$$(F_A)_{\mathrm{eff}}=\eta F_A \tag{29a}$$

and

$$(F_p)_{\mathrm{eff}}=F_p\eta(1+\alpha)\frac{\vec{q}^2+m_\pi{}^2}{(1+\alpha)\vec{q}^2+m_\pi{}^2}\ . \tag{29b}$$

The renormalization factors η and α arise from pion rescattering in the medium. In more realistic models many effects contribute to η and α such as the finite range of the pion-nucleon interaction, short range and long range (Pauli) nucleon-nucleon correlations, intermediate ρ meson production, and surface effects. Thus there is significant model dependence as to whether the effective coupling constants are enhanced or suppressed, depending on the region of the nucleus dominating the process under consideration.

For a process where the three-momentum transfer delivered to the nucleus is small but $q_0\approx m_\mu$, such as the high nuclear final state excitation region of muon capture, Bernabéu *et al.*[9] have used PCAC to go beyond the impulse approximation. In this case one can relate the time component of the axial vector current to the transition pion field matrix element in momentum space, $M(q_0,\vec{q}=0)$, via

$$A_0(q_0,\vec{q}=0)=-if_\pi\frac{m_\pi{}^2}{q_0}\frac{M(q_0,\vec{q}=0)}{m_\pi{}^2-q_0{}^2}\ . \tag{30}$$

Now the question arises as to what should be used for $M(q_0)$. We note

$$M(q_0,\vec{q}=0)\equiv\int dV_x j(q_0,\vec{x})\ , \tag{31}$$

where

$$j(x)=(\partial^\mu\partial_\mu+m_\pi{}^2)\phi(x) \tag{32a}$$

and

$$j(q_0,\vec{x})=\int e^{iq_0x_0}j(x_0,\vec{x})\ . \tag{32b}$$

The quantity $j(x)$ defines the total pion source and, due to pion rescattering in the medium, in general will be a many-body operator in the target nucleon space. Since $\vec{q}$ is assumed to be very small, only the s-wave terms in the pion source current, (31), contribute.

One must be very careful in constructing models for evaluating the transition matrix element, M, since even for small $\vec{q}$, the momentum transferred to the nucleus is very large for proton induced muon production. Thus, as mentioned earlier, one expects the two-nucleon operator parts of j to be important.

For muon production significant contributions arise from the kinematic region $q_0\approx m_\mu$, $|\vec{q}|\lesssim 80$ MeV/c. By working just above muon production threshold, one can essentially work in the region $q_0\approx m_\mu$ $|\vec{q}|\sim 0$. Of course, in this region, the already rare event is further reduced in cross section. However, for illustrative purposes we shall briefly consider this region.

In order to clarify the steps involved in using PCAC and going beyond the impulse approximation for muon production we shall first consider only single nucleon contributions to the source current, j. Thus we write for the transition matrix in Eq. (30)

$$\langle f\,|A_0\,|i\rangle=-i\frac{m_\pi{}^2}{m_\mu}\frac{f_\pi}{(m_\pi{}^2-m_\mu{}^2)}\langle f\,|j_\pi\,|i\rangle \tag{33}$$

and, for j_π, we take

$$j_\pi \to i\frac{g_r}{\sqrt{2}M_p}\left[\vec{\nabla}_\pi + C\vec{\nabla}_p\right]\cdot\vec{\sigma}\ . \tag{34}$$

This yields

$$\langle f\,|\,j_\pi(x)\,|\,i\rangle = (2\pi)^{3/2}e^{-i(\vec{K}_F-\vec{k}_p)\cdot\vec{x}} \times\phi^*_{nljj_z}(\vec{K})\left[\frac{g_r}{\sqrt{2}M_p}\vec{\sigma}\cdot\vec{Q}\chi_{s_p}\right], \tag{35}$$

where

$$Q\equiv\vec{K}_F-\vec{k}_p+Ck_p=\vec{k}_\pi+C\vec{k}_p\ , \tag{36a}$$

$$K=\vec{K}_F-\vec{k}_p+\frac{A}{A+1}\vec{k}_p=\vec{K}_f-\frac{\vec{k}_p}{A+1}\ , \tag{36b}$$

and

$$\vec{k}_\mu+\vec{k}_\nu=\vec{k}_\pi=\vec{k}_p-\vec{K}_f\ . \tag{36c}$$

Note that since $\vec{k}_\mu+\vec{k}_\nu=\vec{k}_\pi\approx 0$ is assumed, that $\vec{k}_p\simeq\vec{K}_f$ and, thus, $\vec{K}_f-\vec{k}_p/A+1$ is, as before, a momentum transfer of several hundred MeV/c. The s wave piece of the pion production operator is included in the term Ck_p, which, for an incident proton of 148 MeV and $C=-m_\pi/m_p$ is ~ 80 MeV/c. Substituting Eq. (31) into (29) allows one to write

$$\langle f\,|\,A_0\,|\,i\rangle\equiv(2\pi)^{3/2}e^{-i(\vec{K}_f-\vec{k}_p)\cdot\vec{x}}\tilde{J}^0\ , \tag{37}$$

where

$$\tilde{J}_0\equiv\phi^*_{nljj_z}(\vec{K})\left[\frac{g_r}{\sqrt{2}M_p}\vec{\sigma}\cdot\vec{Q}\chi_{\rm sp}\right] \times\left[\frac{-im_\pi{}^2f_\pi}{m_\mu(m_\pi{}^2-m_\mu{}^2)}\right]. \tag{38}$$

This expression should be compared with the earlier expressions obtained for A^0 using the impulse approximation. For example, in the impulse approximation the operator appearing in the time component of the axial vector current has the form [see Eq. 9(a)]

$$J_0=-\frac{F_A}{2M_p}\left[\vec{\sigma}\cdot(\vec{k}_p+\vec{k}_n)\right] \tag{39a}$$

$$=-\frac{F_A}{2M_p}\left[\vec{\sigma}\cdot\frac{2A}{A+1}\vec{k}_p\right]$$

$$=-\frac{F_A}{M_p}(\vec{\sigma}\cdot\vec{k}_p)\frac{A}{A+1} \tag{39b}$$

(for $\vec{k}_p=\vec{k}_\nu+\vec{k}_\mu+\vec{K}_F$ and $\vec{k}_\nu+\vec{k}_\mu=0$) ,

where from using PCAC for the target current, in the limit $\vec{k}_\pi=\vec{k}_\mu+\vec{k}_\nu=0$, and $A\to\infty$, we obtain

$$-\frac{g_r}{\sqrt{2}M_p}(\vec{\sigma}\cdot C\vec{k}_p)\frac{m_\pi{}^2f_\pi}{m_\mu(m_\pi{}^2-m_\mu{}^2)}\ , \tag{40a}$$

which, using the Goldberger-Treiman relation $F_A=f_\pi(g_r/\sqrt{2}M_p)$, can be rewritten in the form

$$F_A(\vec{\sigma}\cdot\vec{k}_p)\frac{Cm_\pi{}^2}{m_\mu(m_\pi{}^2-m_\mu{}^2)}\ . \tag{40b}$$

If one chooses a model in which $C=m_\pi/M_p\approx\frac{1}{7}$, the so-called Galilean invariant form for the pion production operator, then one obtains from Eqs. (39b) and (40b)

$$\left|\frac{J_0(\text{PCAC})}{J_o(\text{impulse})}\right|\approx 3\ , \tag{41}$$

thus yielding a predicted order of magnitude enhancement in the cross section for muon production from this term alone. One is accustomed to the time component of the axial vector current being small. In fact, as mentioned earlier, for muon production it is not negligible even in the impulse approximation because the incident nucleon momentum is appreciable [(see Eq. (17)]. It is interesting that the application of PCAC above further enhances the role of the time component of the axial vector current in muon production.

The question of the validity of using a single nucleon model for j_π in describing the high momentum transfer muon production process is directly related to the validity of using a single nucleon j_π to describe threshold pion production. In fact, there does not currently exist a satisfactory theory of threshold pion production; however, theoretical investigations have demonstrated the relative importance of a two nucleon mechanism.[10] In order to obtain a crude estimate of the present calculation's validity for the magnitude of total muon production cross sections, it is necessary to compare plane wave (PW) single-nucleon mechanism pion production calculations with experimental data. Previous PW theoretical estimates[5,11] have demonstrated that (a) there is considerable sensitivity to bound state wave function parameters, and (b) the predicted angular distributions are not satisfactory when compared with experiment (especially at large angles). Nevertheless, the predicted total cross sections appear to be in agreement with experiment (for the Saxon-Woods parameters adopted herein) to within an order of magnitude near $T_p=185$ MeV. For example, at 185 MeV,

Keating and Wills find that in a plane wave model and using a Galilean invariant (i.e., S and P wave production terms are present) single nucleon production operator, the predicted pion production total cross section to the ground state of ^{13}C is $\sim 20\%$ below the observed rate. Of course, the situation could be somewhat different right at and below threshold. However, this result suggests that the main renormalization, assuming a single nucleon mechanism, for the total rate may be the effect coming from using PCAC as already indicated. Use of a more realistic two nucleon mechanism should result in less sensitivity to distorted wave and bound state parameters and allow two particle-one hole final states to be reached. Such states contain a major part of the cross section near threshold.[12] This can result in a further significant enhancement of the total cross section.

The next step in obtaining a more realistic estimate of the muon production rate is to generalize the discussion above to $\vec{q}$, $q_0 \neq 0$, and to go beyond the simple model for j_π given above (by using threshold pion production experimental results). We briefly discuss how this might proceed. Previous investigations[9] assuming PCAC and axial locality[9] have obtained the following results for the time and space components of the axial vector current

$$A_0(q_0,\vec{x}) = -i\frac{f_\pi}{q_0}[\, q_0{}^2\phi(q_0,\vec{x}) + \sigma(\vec{x}) - Q(\vec{x})\phi(q_0,\vec{x})] \,, \tag{42a}$$

$$\vec{A}(q_0,\vec{x}) = f_\pi[-\vec{\nabla}\phi(q_0,\vec{x}) + \vec{\Sigma}(\vec{x}) + \alpha(\vec{x})\vec{\nabla}\phi(q_0,\vec{x})] \,. \tag{42b}$$

The terms appearing in Eq. (42) arise from first using the axial locality assumption to equate the non-pion pole contributions to the time (space) component of the axial vector to the local s wave (p wave) part of the pion source current.[9] The source current is then written as a single nucleon vertex

$$j = \underbrace{\sigma(x)}_{s\text{wave}} - \underbrace{\vec{\nabla}\cdot\vec{\Sigma}(x)}_{p\text{wave}} \,, \tag{42c}$$

plus a rescattering contribution in the medium described by a nonlocal optical potential

$$2m_\pi V = \underbrace{Q(\vec{x})}_{s\text{wave}} - \vec{\nabla}\cdot\underbrace{\alpha(x)\vec{\nabla}}_{p\text{wave}} \,. \tag{42d}$$

The important result of separating the s and p wave contributions into the time and space components allows one, for example, to relate the time component of the axial vector current in the many body medium to s wave pion production experimental information—even when $\vec{q}$ is nonzero. Of course, the validity of the extra assumption concerning axial locality, while perhaps reasonable at low q, remains to be experimentally investigated. In principle, other processes such as neutrino induced muon production, large nuclear energy excitation muon capture, and radiative muon capture are potential sources of information about the axial time component and, more generally, the assumption of axial locality.

The original arguments[9] motivating the axial-locality assumption noted that there would be concern if the hypothesis were used in situations where one was sensitive to two nucleon correlations, etc. (i.e., a sensitivity to the short range scale in the nucleus). Presumably this would naturally exclude processes where the axial current is required at a three-momentum transfer significantly above the Fermi momentum and/or the initial and final nuclear states differ by the quantum numbers of two or more nucleons. In the case of the muon production process under consideration, there is the complicating feature that although one requires the axial vector current at low $\vec{q}$ ($<< k_F$) the momentum transfer to the nucleus is quite large ($> 3/2K_F$) so that a two nucleon process may be favored. Of course a theoretical calculation of the two nucleon mechanism in large energy loss weak interactions is required. Such investigations are underway. Note the reliability of the two-nucleon mechanism calculations can be tested by first successfully predicting threshold pion production. This appears to be a challenging hurdle. We discuss proposed further research associated with this point in Sec. IV.

III. RESULTS

Using Eq. (15) and the subsequent relations, Eqs. (16)–(21) and procedures described in the previous section we have calculated muon production cross sections for ($T^P_{\text{lab}} = 148$ MeV) protons incident on ^{12}C. The expression and numerical values associated with the muon and proton wave function renormalizations and final neutron single particle potential are given in Sec. II. For the purpose of these estimates we adopt the simple structure model, where ^{12}C consists of closed $1s_{1/2}$ and $1p_{3/2}$ shells and the states of ^{13}C consist of the closed core plus

a valence neutron in an orbital having the quantum numbers of the state under consideration. Typical angular distributions are shown in Fig. 1 for a bound $1d_{5/2}$ state. The general forward peaking of the cross section and the behavior of the cross section as a function of muon momentum is similar for all the bound states. The differential cross section associated with $k_\mu \approx 60$ MeV/c ($T^{\mu}_{\rm lab} = 21$ MeV) is predicted to be the largest in magnitude at angles $\lesssim 90°$. This characteristic is also shared with muon production leading to other bound states. The relative size of the predicted cross sections for bound $1p_{1/2}$, $2s_{1/2}$, and $1d_{5/2}$ states are shown in Fig. 2 for $k_\mu = 60$ MeV/c using both harmonic oscillator (ho) and Saxon-Woods single particle orbitals. Since there is a node in the momentum space single particle Saxon-Woods wave function in the region 475–600 eV/c (not present for ho orbitals) it is not always true that such wave functions give a bigger cross section than the ho orbitals yield at large momentum transfer. We note there is considerable state and single particle-orbital dependence in the magnitude of the predicted cross sections. This is associated with the considerable dependence of the cross section on high momentum components in the single particle wave functions. Such sensitivity naturally occurs in a one step mechanism involving large momentum transfer and is expected to be significantly reduced when more realistic multistep mechanisms are included.

The impulse approximation predicted cross sections are quite low for individual states and particular values of the muon momentum. Thus in the following, we sum over the available muon energy. In Fig. 3 we present the summed-muon-energy angular distributions for the three (assumed) single particle bound states and the impulse total bound contribution.

The energy integrated cross sections shown in Fig. 3 retain the forward peaking seen earlier for particular energies (see Figs. 1 and 2). In addition the less bound states (with higher single particle energy) contribute much more to the total cross section than the $1p_{1/2}$ ground state. Artificially

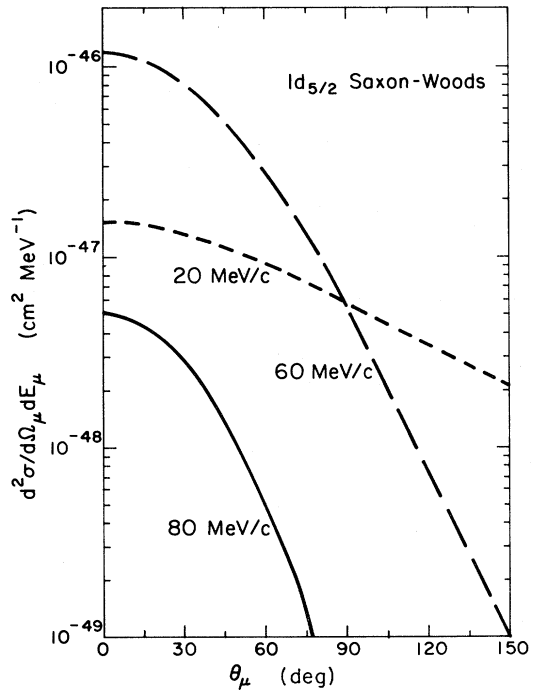

FIG. 1. Angular distributions for proton-induced muon production on ^{12}C leading to the lowest $\frac{5}{2}^+$ state of ^{13}C for different muon final momenta. A Saxon-Woods $1d_{5/2}$ single nucleon orbital and the simple impulse approximation have been utilized. The incident energy of the proton is taken to be 148 MeV.

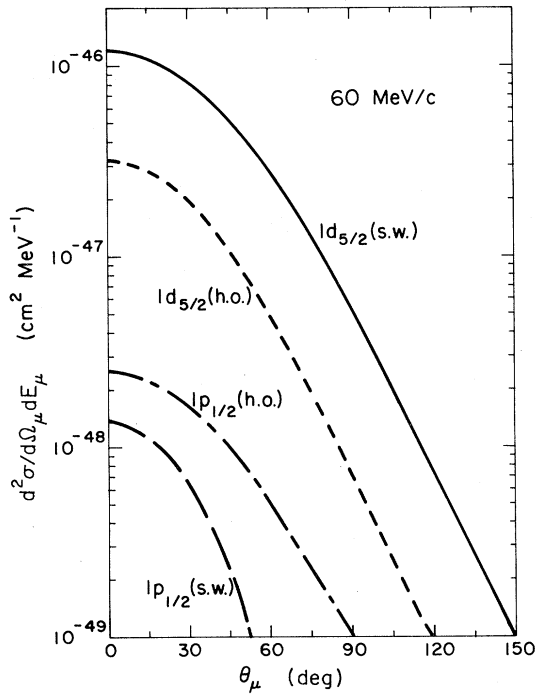

FIG. 2. Same reaction as Fig. 1, but here the angular distributions associated with the lowest $\frac{5}{2}^+$ and the g.s. ($\frac{1}{2}^-$) of ^{13}C are shown for a final muon momentum of 60 MeV/c. We compare the results associated with using harmonic oscillator (ho) or Saxon-Woods (SW) orbitals for the valence neutron.

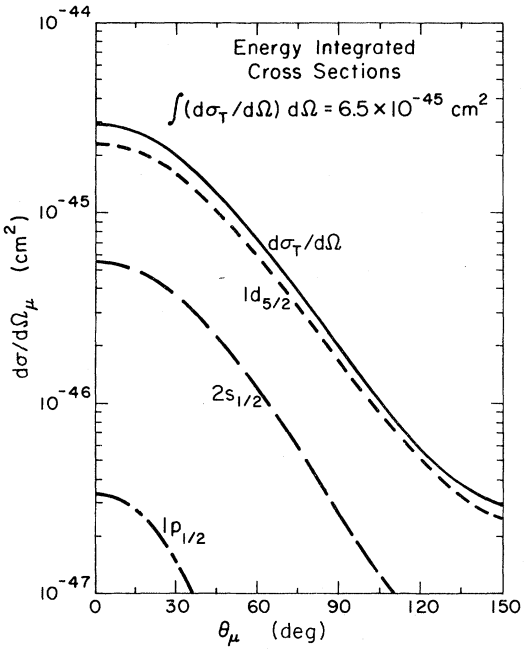

FIG. 3. The muon-energy-summed angular distributions for the lowest $\frac{1}{2}^-$, $\frac{5}{2}^+$, and $\frac{1}{2}^+$ states of ^{13}C formed in 148 MeV proton induced muon production from ^{12}C. Saxon-Woods orbitals and the impulse approximation were adopted. The sum of the three angular distributions $d\sigma_T/d\Omega$ as well as the angle integrated total bound state contribution $\int(d\sigma_T/d\Omega)$ are also indicated.

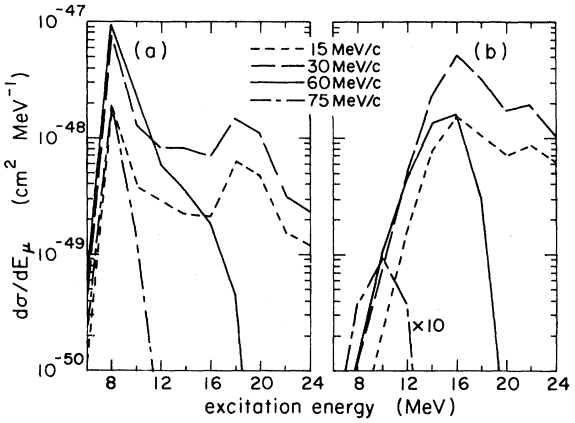

FIG. 4. The angle integrated and muon-energy integrated cross sections for (a) the continuum $d_{3/2}$ neutron partial wave and (b) the continuum $f_{7/2}$ neutron partial wave are shown as a function of nuclear excitation energy. A Saxon-Woods well has been assumed. Details of the continuum calculation are given in the text. The reaction is the same as in Fig. 1.

binding the $1f_{7/2}$ and $1d_{3/2}$ states would result in the prediction that these states dominate the total capture rate. If these two states are included more carefully in the continuum calculation their predicted contribution is greatly decreased (see below). The $1d_{5/2}$ state contribution contributes $\approx 80\%$ to the total $(d\sigma/d\Omega_T)$ single particle bound state contribution. After angle integrating the total energy-integrated bound state cross section one obtains a prediction for the total bound state capture rate of 6.5×10^{-45} cm^2.

To obtain the total capture rate, the continuum contribution must be included. We show in Figs. 4(a) and 4(b) the excitation energy dependence of the two largest contributions to the continuum production cross section. The peaks in the muon (momentum and angle integrated) continuum cross sections are associated with excitation energies, where the given continuum wave function has its greatest probability in the nuclear well (near a positive energy resonance). The excitation energy-integrated continuum cross section for the combined $1d_{3/2}+1f_{7/2}$ continuum single particle functions is 0.8×10^{-45} cm^2. The total continuum calculated cross section in the impulse approximation is 1.2×10^{-45} cm^2. Combining this result with the earlier determined bound state cross section yields a total (summed angle, energy, and nuclear state) cross section of 7.7×10^{-45} cm^2. To obtain the total continuum calculation we have calculated, through $l=6$, the individual partial wave contributions. (The $l=5$ and $l=6$ contributions are more than three orders of magnitude smaller than the dominant $1d_{3/2}$ continuum contributions.) The nuclear excitation energy region included in the calculations goes from neutron threshold to approximately 24 MeV where energy and momentum conservation constraints impose an upper bound. Note that the single nucleon continuum contribution while non-negligible is not dominant. Including higher partial waves and artificially binding the resulting positive energy eigenstates would lead to a substantial overestimate of the impulse cross section because of the sensitivity to the higher partial wave single particle orbital high momentum components.

In order to obtain an estimate of the impulse approximation total counting rate we use the relationship

$$\text{number/sec} = \frac{3.76}{A}(T)I\ , \tag{43}$$

where

$\sigma \equiv$ total cross section (mb) ,

$T \equiv$ target thickness (μg/cm^2) ,

$I \equiv$ beam current (nA) ,

$A \equiv$ atomic weight of target nucleus .

Although one may expect significant enhancement in beam currents in the future, it is useful to obtain a lower bound on the counting rate to be expected using presently available experimental parameters and the impulse approximation theoretical prediction. Thus we assume a ^{12}C target thickness $T \approx 150$ mg/cm^2, beam current I of 10 μA, and a cross section, σ, of 10^{-44} cm$^2 = 10^{-11}$ mb. Using Eq. (43) this results in $\sim \frac{1}{2} \times 10^{-8}$ counts/sec or ~ 1 count/decade. A two orders of magnitude enhancement of the counting rate which might be reasonable from the discussion in Sec. II would result in ~ 1 count/month.

IV. DISCUSSION

We have studied the weak process $p + {}_zA \rightarrow {}_z(A+1) + \mu^+ + \nu$ using the impulse approximation, the usual *V-A* theory of weak interactions, and a simple single particle shell model for the required nuclear structure. In the specific example chosen (148 MeV protons incident on ^{12}C), the total cross section for all energetically available single particle bound and continuum states is 7.7×10^{-45} cm^2. This yields a counting rate too low to be practical with existing experimental parameters. However, we suggest that the reaction is quite interesting and that the simple impulse approximation provides a lower bound for the counting rate with the total actual rate being perhaps one to two orders of magnitude greater. We elaborate on these points in the discussion below.

We remarked earlier that there are two momenta of interest in the problem, (1) the momentum transfer at which the intrinsic nuclear-transition density (form factor) is evaluated, and (2) the four-momentum $(\vec{q}, q_0)$ values for which one requires the nuclear vector and axial vector weak current. Since a medium energy proton, just below threshold for producing real pions, is incident on the nucleus, the initial nucleon momentum is substantial. Most of the initial energy of the nucleon goes into making the muon mass. The small amount of energy remaining is most efficiently used up in final total nuclear target recoil. Thus the muon and neutrino possess little momentum ($q < q_0 \sim m_\mu$) and the weak axial and vector currents are to be evaluated at low three momentum transfer but at an energy transfer much higher than realized in beta decay or in the main contributions to muon capture. The momentum transfer at which the nuclear transition density is evaluated has a value of approximately twice the fermi momentum. These simple kinematic considerations result in the following:

(1) The impulse approximation results are very sensitive to uncertainties in the high momentum components of required nuclear wave functions.

(2) The time component of the axial vector current plays a relatively more important role than in usual muon capture or beta decay.

(3) Just as in the high nuclear energy excitation part of muon capture one does not expect the impulse approximation result for the fourth component of the axial vector current to be reliable for $q_0 \approx m_\mu$. Following Ericson and co-workers we show that a simple application of PCAC results in an order of magnitude increase in the predicted counting rate (associated with fourth component of the axial vector current) *even* when a one nucleon mechanism is assumed for the related subthreshold pion production transition operator.

(4) Independent of the expected failure of the impulse approximation discussed in (3) the high momentum transfer delivered to the nucleus should result in the relative importance of "two step" nonimpulse processes involving two nucleons. Thus one expects the strong excitation of particular two particle-one states in ^{13}C. Such states [3.68 ($\frac{3}{2}^-$), 6.86 ($\frac{5}{2}^+$), and 9.50 ($\frac{9}{2}^+$) MeV] are strongly seen[12] in threshold pion production from ^{12}C. In fact, the total cross section to the $\frac{9}{2}^+$ state is greater than any of the single particle state cross sections (for pion production) and thus inclusion of the two nucleon mechanism allowing excitation of such states should further significantly enhance the muon production counting rate.

The same kinematic related problems discussed above are also present for intermediate energy (p,γ) and (p,π) reactions. These reactions are intimately related to (p,μ) via conserved vector current (CVC) and PCAC, respectively. The (p,μ) reaction contains information on the validity of the assumptions of axial locality and, potentially the importance of transverse contributions to the axial vector current. Whether the process will become experimentally practical to study in the *near* future is not clear.

Perhaps a relatively simple initial experiment would involve measuring the muon counting rate

associated with a (p,π) experiment. One could start initially a few MeV above threshold (where the muons come from real pions decaying in flight) and lower the proton energy until one is below real pion production threshold. Although the results of the present *impulse approximation calculation* indicate the total rate below threshold would be prohibitively low with present experimental parameters, it is desirable to have this easily obtainable experimental check, especially in view of the potential importance of, and present lack of information regarding, two nucleon mechanisms near pion production threshold.

This work was supported in part by the U. S. Department of Energy and the National Science Foundation.

---

*Present address: Theoretical Applications Division, Los Alamos Scientific Laboratory, Los Alamos, New Mexico 87544.

†Address while on sabbatical leave 1980-81, Institute for Nuclear Theory and Physics Department, University of Washington, Seattle, Washington 98195.

[1]As examples, M. Chemtob and M. Rho, Nucl. Phys. A163, 1 (1971); J. Delorme, M. Ericson, A. Figureau, and C. Thevenet, Ann. Phys. (N.Y.) 102, 273 (1976); F. Dautry, M. Rho, and D. O. Riska, Nucl. Phys. A264, 507 (1976); E. Ivanov and E. Truhlik, *ibid.* A316, 437 (1979); W. K. Cheng and B. Goulard, Phys. Rev. C 28, 869 (1981).

[2]Z. Grossman, F. Lenz, and M. P. Locher, Ann. Phys. (N.Y.) 84, 348 (1974); A. Reitan, Nucl. Phys. A237, 465 (1975); M. Dilling and M. G. Huber, Phys. Lett. 69B, 429 (1977); H. Hebach, M. Wortberg, and M. Gari, Nucl. Phys. A267, 425 (1976); J. T. Londergan, G. D. Nixon, and G. E. Walker, Phys. Lett. 65B, 427 (1976); J. T. Londergan and G. D. Nixon, Phys. Rev. C 19, 998 (1979).

[3]J. D. Bjorken and S. D. Drell, *Relativistic Quantum Fields* (McGraw-Hill, New York, 1965).

[4]J. T. Londergan and G. D. Nixon, Phys. Rev. C 19, 998 (1979).

[5]M. P. Keating and J. G. Wills, Phys. Rev. C 7, 1336 (1973).

[6]T. W. Donnelly, Nucl. Phys. A150, 393 (1970).

[7]L. I. Schiff, *Quantum Mechanics,* 3rd ed. (McGraw-Hill, New York, 1968), p. 141.

[8]J. Delorme *et al.,* Ann. Phys. (N.Y.) 102, 273 (1976).

[9]T. E. O. Ericson, Centre European de Recherches Nucleaires (CERN) Report No. TH2257, 1976; J. Bernabeu, T. E. O. Ericson, and C. Jarlskog, CERN Report No. TH2301, 1977; and T. E. O. Ericson and J. Bernabeu, CERN Report No. TH204, 1977.

[10]See, for example, the first and third articles listed under Ref. 2.

[11]B. Hoistad, S. Dahlgren, P. Grafström, and A. Asberg, Phys. Scr. 9, 201 (1974).

[12]F. Soga, P. H. Pile, R. D. Bent, M. C. Green, W. W. Jacobs, T. P. Sjoreen, T. E. Ward, and A. G. Drentje, Phys. Rev. C (to be published).